Pre-Maximum Spectropolarimetry of the Type Ia SN 2004dt [1]

Lifan Wang[1,2], Dietrich Baade[3], Peter Höflich[4], J. Craig Wheeler[4], Koji Kawabata[5], Alexei Khokhlov[6], Ken'ichi Nomoto[7], Ferdinando Patat[3]

[1]*Purple Mountain Observatory, 2 West Beijing Road, Nanjing 210008, China*

[2]*Lawrence Berkeley National Laboratory, 1 Cyclotron Rd, Berkeley, CA 94712*

[3]*European Southern Observatory, Karl-Schwarzschild-Strasse 2, D-85748 Garching, Germany*

[4]*Department of Astronomy and McDonald Observatory, The University of Texas at Austin, Austin, TX 78712*

[5]*Astrophysical Science Center, Hiroshima University, 1-3-1 Kagamiyama, Higashi-Hiroshima, Hiroshima 739-8526, Japan*

[6]*Department of Astronomy, Department of Astronomy and Astrophysics, University of Chicago, Chicago, Illinois 60637, USA*

[7]*Department of Astronomy, University of Tokyo, Bunkyo-ku, Tokyo 113-0033, Japan*

ABSTRACT

We report observations of SN 2004dt obtained with the Very Large Telescope of the European Southern Observatory on August 13.30, 2004 when the supernova was more than a week before optical maximum. SN 2004dt showed strong lines of O I, Mg II, Si II, and Ca II with typical velocities of absorption minimum around 17,000 km s^{-1}. The line profiles show material moving at velocities as high as 25,000 km s^{-1} in these lines. The observations also reveal absorption lines from S II and Si III with a velocity of only 11,000 km s^{-1}. The highest velocity in the S II features can be traced no higher than 15,000 km s^{-1}, much lower than those of O, Mg, Si, and Ca. SN 2004dt has a polarization spectrum unlike any previously observed. The variation of the polarization across some Si II lines approaches 2%, making SN 2004dt the most highly polarized SN Ia ever observed. In contrast, the strong line of O I at 777.4 nm shows little or no polarization signature. The degree of polarization points to a richly-structured partially burned silicon layer with substantial departure from spherical symmetry. A geometry that would account for the observations is one in which the distribution of oxygen is essentially spherically symmetric, but with bubbles of intermediate-mass elements with significant opacity within the oxygen substrate.

Subject headings: supernovae – cosmology – spectropolarimetry

1. Introduction

As for core-collapse supernovae, high-quality spectropolarimetry of Type Ia Supernovae (SNe Ia) is revealing a complex array of behavior that has opened a new window of exploration of this class of explosions (Wang et al. 1996; Wang, Wheeler, Höflich 1997; Howell et al. 2001; Wang et al. 2003a; Wang et al. 2004). While there are indications that the degrees of polarization of core-collapse supernovae increase with time after explosion (Wang et al. 2001, 2002; Leonard et al. 2001), the time evolution of Type Ia supernovae seems to be rather different (Wang et al. 2003a).

Polarimetry of SN Ia shows that the degree of polarization of normal SN Ia is $\lesssim 0.3\%$, which is much lower than the typical polarization of core-collapse supernovae (Wang et al. 1996). Spectropolarimetry of the normally-bright SN 1996X at optical maximum tentatively showed intrinsic polarization of about 0.3% which implies geometrical asphericities of about 10% (Wang et al. 1997). Hydrodynamic instabilities just beyond the layers of complete thermonuclear equilibrium may have contributed to the polarization signal from SN 1996X. Howell et al (2001) showed that SN 1999by, a sub-luminous SN Ia, was polarized at a level of 0.7% in the red continuum.

The observations of the normally-bright SN 2001el revealed the geometrical structure of an SN Ia in different chemical layers. The degree of polarization showed significant time evolution (Wang et al. 2003a). An exceedingly strong Ca II feature at velocity of 20,000 - 26,000 km s^{-1} was highly polarized. This feature showed that the outermost layers of the supernova ejecta had a highly aspherical geometry (Wang et al. 2003a; Kasen et al. 2003). Deeper inside the ejecta, the silicon-rich layer also displayed asphericity as evidenced by the detection of polarization of $\sim 0.3\%$ for the Si II 635.5 nm line. When the photosphere receded deep inside the iron-rich layers, the polarization diminished and the supernova appeared spherical. Wang et al. listed several possible origins of this asymmetric high-velocity material: matter from a disk or companion star that is swept up by the supernova ejecta; newly-synthesized material produced by thermonuclear reactions in the high velocity collision between supernova ejecta; and a clump of matter ejected from the intrinsic thermonuclear combustion process. Gerardy et al. (2004) examined the high-velocity Ca II feature in SN 2003du (for

[1]Based on observations collected at the European Southern Observatory, Chile (ESO Progr. No. 073.D-0565(A)).

which there was no spectropolarimetry) and concluded that the strength of the Ca II in that event was consistent with solar abundance of calcium in a hydrogen plasma (that the bulk of the matter was helium or carbon/oxygen cannot be ruled out) that was swept up from distances consistent with the expected separation of the companion star.

We present in this paper observations of SN 2004dt. This event showed exceptionally strong and broad lines of Si II, and O I and revealed the strongest polarization signal we have yet measured for a SN Ia. The discovery and pre-maximum observations are described in §2, the spectral and spectropolarimetry features and their implications for ejecta geometry are discussed in §3. A brief discussion and conclusions are presented in §4.

2. Discovery and Observations

SN 2004dt in NGC 799 was discovered on an unfiltered image taken on August 11.48 at a magnitude of about 16.1 (Moore & Li 2004). Salvo, Schmidt & Wood (2004) reported that a spectrum taken on August 12.72 UT showed SN 2004dt to be a young SN Ia a few days before maximum light. The photospheric expansion velocity deduced from the absorption minimum of Si II 635.5 nm was about 16,500 km s^{-1}, adopting the recession velocity of 5915 km s^{-1} reported by the NED for the host galaxy NGC 799. Patat, Pignata, and Benetti (2004) reported that a spectrum obtained on Aug. 13.17 UT showed some unusual features. They noted that the O I 777.4 nm transition was particularly pronounced, with a broad symmetric P-Cygni profile and also had an expansion velocity of about 16,800 km s^{-1}. They also report that the Ca II H & K line gave 22,200 km s^{-1} (we think this feature is mostly due to a Si II line, see §3.2). Patat, Pignata, and Benetti (2004) suggested that the high velocities of the lines indicated a very early phase. They noted that other intense lines visible in the spectrum were from Fe III and Si III.

We observed SN 2004dt with the ESO-VLT on 2004 August 13.30 with the FORS1 instrument in polarization mode. From preliminary light curves of Li et al. (2004, private communication), this corresponds to 6-8 days before optical maximum. Four exposures of 1200 second durations were taken with the waveplate at position angles of 0, 45, 22.5, and 67.5 degrees. Flux and polarization standard stars were observed to calibrate the flux levels and polarization position angles. The data were reduced in a way similar to that described in Wang et al. (2003a).

Figure 1 shows the total flux spectrum, the polarization, the Stokes parameters and the polarization angle. The degree of polarization is corrected for biases due to observatinal noise using the equations derived in Wang, Wheeler, & Höflich (1997). There are many distinct

features in the total flux spectrum, as noted by Patat, Bignata & Benetti (2004). Starting in the blue, there is no sharp drop of flux blue ward of the strong Ca II H & K absorption as observed in normal SN Ia at optical maximum. The Ca II H & K feature appears very strong although, as we argue in §3.2, it is probably significantly affected by Si II. The strong line of Si II 635.5 nm shows the typical blue-shifted absorption that characterizes SN Ia at 600 nm, but it is especially strong, broad, and fast moving. The minimum corresponds to a velocity of about 17,000 km s^{-1}, and the blue wing extends to about 25,000 km s^{-1}. We also observe a strong line of O I 777.4 nm as pointed out by Patat, Pignata, and Benetti (2004). This line also showed an absorption minimum at about 17,000 km s^{-1} with a the blue wing again extending to about 25,000 km s^{-1}. To first order, the Si and O occupy the same velocity and hence radial space. Our data show two components of the Ca II IR triplet, a broad absorption at 820 nm and a "notch" indicating a separate, high-velocity component at about 800 nm. These represent velocities of $\sim$ 16,000 and 23,000 km s^{-1}, respectively. The lower velocity component corresponds approximately to the velocity minimum of Si II and O I. The higher velocity component seems kinematically distinct as in SN 2001el (Wang et al. 2003a) and SN 2003du (Gerardy et al. 2004) and to correspond roughly to the blue wing of the Si II and O I lines. Despite the likely two-component nature, the highest velocity, again, can be traced to 25,000 km s^{-1} for Ca II IR triplet, similar to the other high velocity lines.

The strong absorption feature at 421 nm is due to Mg II 448.1 nm, blended with Fe III and Si III lines. If this feature is predominantly Mg II, then the absorption minimum of the Mg II line is blueshifted by 17,000 km s^{-1}, consistent with the lines of Si II, Ca II, and O II.

The absorption minima of the S II "W" lines are measured to be at 523.5 and 543.1 nm which implies a velocity of only 11,000 km s^{-1}. This is significantly lower than the velocity of the Si II lines. Weak lines at 439.5, 454.2, and 464.0 nm, tentatively identified with Si III 456.0 nm, S II 471.6 nm, and S II 481.6 nm, respectively, also show the much lower velocity of 11,000 km s^{-1}. The presence of Si III 456.0 nm at 11,000 km s^{-1}, not at 17,000 km s^{-1} shows that doubly ionized Si exists only close to the central region.

The second, third, and fourth panels of Figure 1 show the polarization, P, and the reduced Stokes vectors, U, and Q. The Q vector, in particular, shows a total excursion of $\sim$ 2 percent with sharp wavelength dependence, indicating strong, intrinsic polarization. The bottom panel of Figure 1 gives the polarization angle. It is nearly constant from 330 nm to 630 nm, but then shows a strong change with possibly significant excursions at wavelengths longer than 630 nm. This change could be due to a combination of polarization by interstellar dust and the intrinsic polarization by the supernova ejecta. Note that the "spikes" in the polarization angle at wavelengths longer than 630 nm return to approximately the same

angle as the shorter wavelength data, $\sim 150^{o}$.

Figure 2 gives the data in the Q/U plane where each point represents the Stokes parameters rebinned to 25 Å intervals. The bin size was chosen to be larger than the spectral resolution to minimize correlations among neighboring lines. The total excursion is nearly 3 percent. The scatter of points is predominantly due to line features. The data points span a range of about 1.5 percent in Q and more than 2 percent in U. Figure 2 shows that the bulk of the points fall along the line that represents the "dominant axis" of the geometry (Wang et al. 2001), determined by making a principle component decomposition of the data points on the Q/U plane. The scatter orthogonal to this axis suggests that there are smaller but real deviations in the geometry from this dominant axis that may also constrain the physics of the explosion.

3. Interpretation

3.1. The Distinguishing Spectral Features

The colors synthesized from the spectrum give $U-B \sim$ -0.6. This blue color (as verified by the strong blue flux in Figure 1), suggests that this event, if approximately "normal," is close to or before U maximum. This may mean that at this phase, SN 2004dt has not yet been subject to the strong line absorption leading to the characteristic UV deficit of normal SN Ia near maximum light (Wheeler & Harkness 1992; Kirshner et al. 1993). The blue $U-B$ color is also consistent with the absence of strong Fe II features of the spectrum.

The strong lines of Si II 635.5 nm and O I 777.4 nm in the total flux spectrum suggest that there is substantial ejected silicon and oxygen, moving at velocities approaching 25,000 km s^{-1}. This would be consistent with a significant mass of incompletely burned matter. The lack of a UV deficit suggests that there is not much iron in the photosphere at the phase of these observations, or that the photospheric temperature is high.

The presence of lines at a velocity of 11,000 km s^{-1} suggests that even at this early phase, the ejecta is not Thompson opaque at this lower velocity. The velocity of the Si III 455.3, 456.8, and 457.5 blend is only 11,000 km s^{-1}, implying that doubly-ionized silicon exists mainly in this lower-velocity region. The low velocity S II line suggests that S is more concentrated in the low-velocity region than Ca, O, Mg, and Si.

3.2. The Interstellar Polarization of SN 2004dt

From the strong modulation of the raw polarization shown in Figure 1 it is immediately evident that the intrinsic linear polarization of SN 2004dt is exceptionally large. The vectorial nature of polarization can lead to questionable conclusions if the interstellar polarization (ISP) is not properly determined and subtracted; unfortunately, this almost inevitably requires some assumptions. We have tried to avoid assumptions that are tied to the physics of SN Ia explosions.

The central assumption made is that the ISP dominates where the continuum polarization of the supernova is the lowest. The effective continuum polarization probably gets decreased by overlapping spectral lines. Since there are many more such lines in the blue portion of the spectrum (they are mostly due to Fe II) than in the red portion (Wang et al. 2001; Howell et al. 2001; Wang et al. 2003a), we have selected the regions marked in Figures 1 and 2; they avoid significant discrete spectral features.

It is seen in Figure 2 that the deduced ISP corresponds to $0.2\pm0.1\%$ in Q and $-0.2\pm0.1\%$ in U. This low value is consistent with the absence of an interstellar Na I D line (§3.6) if the gas-to-dust ratio of the host galaxy is normal; the latter condition may not be fulfilled if the reddening is above average as the photometry available suggests (§3.6).

In Figure 2, the data points used for the determination of the ISP are embedded in a large cloud of other low-polarization wavelength bins. If, following Wang et al. (2001), a principle-components decomposition technique is used to define the dominant and the orthogonal polarization axis, the ISP will, therefore, be close to the dominant axes. As Wang et al. (2001) have shown, some minor error in the determination of the ISP does not grossly distort a qualitative interpretation if the true ISP is close to the dominant axis.

A similar constellation of data points prevailed in SN 2001el (Wang et al. 2003a). The key corroborating observation was that at later phases the polarization of the continuum as well as of spectral features retreated along the dominant axis and, starting a week after maximum, remained within a similar cloud of low-polarization wavelength bins. A preliminary analysis of later-epoch data of SN 2004dt shows a similar behavior.

The resulting ISP-corrected decomposition into dominant and orthogonal axis is presented in Figure 3.

3.3. The intrinsic polarization of SN 2004dt

Ultimately, the choice of interstellar polarization must depend on the totality of observations and a self-consistent picture of the physics of the explosion and radiative transfer through the complex ejecta. Important details of the interpretation of the data may yet depend on the particular placement of the ISP. For this paper we have attempted to restrict our discussion to features that are relatively independent of the choice of the ISP.

SN 2004dt shows a polarization spectrum unlike any SN Ia yet observed. Compared to the well-observed SN 2001el, the Si lines are especially prominent in the polarization spectrum, but the lines of the Ca IR triplet are less so.

With the above choice of the interstellar polarization, we see from Figure 3 that the absorption minima of the P-Cygni profiles correspond in general to the peaks of the spectropolarization profiles. Along the dominant axis polarization spectrum, the polarization in the range 620 - 720 nm is around -0.3% for the choice of interstellar polarization adopted in Figure 3. This wavelength range shows no strong spectral lines and it is likely that continuum polarization by Thompson scattering dominates this wavelength region.

There is a strong spike in the polarization at 365.0 nm, the location of the "Ca H & K" line. We suspect this is due primarily to Si II 385.0 nm that is blended with the Ca lines. Note that the amplitude of this polarization feature, $\sim 2\%$, is nearly identical to that of the Si II 635.5 nm line. No other features in the polarization spectrum show this level of polarization. The dominant-axis spectrum shows another feature at 390 nm that we attribute to Si II 413.0 nm. Note, however, that the same feature was tentatively identified as C II 426.7 nm with an expansion velocity of about 24,100 km s^{-1} by Patat et al. (2004). Our identification with Si II would put the line at the same velocity of 17,000 km s^{-1} as the other Si II lines. We note the importance of C II as a diagnostic of the quantity of unburned matter (Marion et al. 2003) and stress that care should be taken in studies of this event to determine the presence or absence of carbon.

The polarization feature at 420 nm is mostly due to Mg II 447.1 nm. The line at 480 nm is due to the blend of Si II 504.1, 505.6 nm, and Fe II 491.3, 501.8, 516.9 nm. As can be seen in Figure 3, the contributions from Fe II must be small as evidenced by the absence of the strongest Fe II line in this wavelength region, Fe II 516.9 nm in the total flux spectrum. The small feature at 570 nm is likely to be due to Si II 595.8,597.9 nm. To the red of the Si II 635.5 nm line, the polarization dips and is then constant to about 720 nm. With these identifications, all the Si II lines have velocities from 15,000 to 17,000 km s^{-1}. The lines of Si II 413 nm, Mg II 447.1 nm, and Si II 504.1, 505.6 nm all have polarization $\sim$ 1% in Figure 3, significantly less than the strongest polarized lines of Si II, but suggesting

some commonality in their geometry. All these lines have similar position angles. Weaker lines from Si III, and S II are also polarized, at a level of about 0.3%, but with polarization position angles similar to those of the other lines.

The polarized spectral feature at 820 nm is clearly due to the Ca II IR triplet. The absorption minimum of the Ca II feature shows a velocity of 16,000 km s^{-1}, consistent with that of the Si II lines. Note that, unlike SN 2001el which showed a highly polarizing detached Ca II shell at a velocity of 22,000 km s^{-1}, the high-velocity component of the Ca II IR triplet of SN 2004dt with a similar velocity is not particularly strong nor does it have an especially high polarization. SN 2001el and SN 2004dt are distinctly different in this regard. The lower velocity component of the Ca II IR triplet in SN 2004dt shows a polarization spike of about 0.7-2%, comparable to the Mg II line. The higher velocity component shows a spike of about 0.3%, comparable to the S II and Si III lines. These polarized components of Ca II seem to share approximately the same polarization angle as all the other polarized lines, $\sim 150^{o}$.

Despite the very strong line of O I in the total flux spectrum, there is little sign of that feature in the polarization spectrum. This is in sharp contrasts to all the other strong lines from Mg II, Si II, and Ca II.

3.4. The Co-existence of Burned and Unburned Material

The null detection of polarization across the O I 777.4 nm line demands an explanation. From the spectral profile, we know that the oxygen co-exists with silicon, magnesium and calcium. Why does not the O I 777.4 nm line share the same polarization properties of lines from the other elements?

A simple explanation is that oxygen is distributed in a different way from silicon, although they share the same velocity space. Oxygen is likely more pervasive in the outer layer, but the products from nuclear burning are distributed in holes or filaments in this region. In such a geometry, the polarization from oxygen and the other elements are drastically different as their geometrical structures are not identical but occupy different regions.

If so, then the null detection of polarization across the O I 777.4 nm line implies that the oxygen layer is not as highly distorted as the silicon rich bubbles. This would require that the silicon rich bubbles also contain a significant amount of oxygen so that oxygen appears to be more "spherically" distributed. This is consistent with the presence of magnesium in these bubbles. In explosive carbon burning, unburned oxygen is expected to co-exist with magnesium, a principal burning product.

In the geometry described above, one expects O I lines to be of significantly lower polarization than the strong Si II lines, but with the position angle of the polarization flipped by 90 degrees. In fact, at 1-sigma level, the OI 777.4 polarization is indeed negative, as compared to the positive spikes of the polarizations of strong Si II lines.

The observed high degree of polarization of magnesium suggests that the silicon rich bubbles are from explosive carbon burning. The fact that it is polarized in the same way as the silicon lines also shows that magnesium is confined into these bubbles. This in turn, suggests that the oxygen outside the bubbles is the unburned oxygen from the progenitor white dwarf.

3.5. The Inferred Ejecta Geometry

To summarize the observed properties, we have found from these observations: (1) Lines of Mg II, O I, Ca II, and Si II are at the highest velocities, their absorption minima are typically blue shifted by 17,000 km s^{-1}, and the lines can be traced to a velocity as high as 25,000 km s^{-1}; (2) The S II lines have absorption minima at only 11,000 km s^{-1}; the highest velocity of these features is less than 15,000 km s^{-1}; (3) The absorption minimum of the Si III 455.3, 456.8, and 457.5 blend is blue shifted by 11,000 km s^{-1}; (4) All the high-velocity features except that from O I 777.4 nm are significantly polarized, at levels from 0.7% to 2.2% with two features of Si II being especially distinct; (5) Weak lines from S II, and Si III are also polarized, at a level of about 0.3%, but share the same polarization position angles as those of the other polarized lines; (6) the high-velocity shell of Ca II has a velocity comparable to the blue wings of the strong lines, but with a polarization amplitude and angle comparable to S II, and Si III.

We believe that the unusual polarization of SN 2004dt is closely related to the observed velocity structures of the various ions. The velocity bifurcation of spectral lines implies that in the outermost portions, a layer of unburned oxygen co-exists with a dense layer of newly synthesized Si, Mg, and Ca. This outermost layer moves at a velocity around 17,000 km s^{-1} and the highest velocity approaches 25,000 km s^{-1}. The silicon rich layer extends deep inwards to velocity of around 11,000 km s^{-1}, as evidenced by the presence of Si III line at that velocity. The broadness and unusually high blueshift of the Si II lines are evidences of that these lines are optically thick. Iron and sulfur are noticeably absent in this layer. The strong polarization observed across the P-Cygni lines of the newly-synthesized elements is the result of the clumpiness of this layer. The polarization position angles of these lines are similar, suggesting that they share the same geometrical structure.

The structure of the ejecta is sufficiently clumpy or fragmented that spectral lines can be formed in significantly different velocity regions. The attribution of the polarization to clumpiness requires the clumps to have considerable radial extent because the polarization angle is the same for lines formed at different depths, that is, both Si II at 17,000 km s^{-1} and Si III at 11,000 km s^{-1}. The photosphere in the conventional sense of Thompson optical thickness probably has a complicated geometry that will complicate attempts to understand the radiative processes. For simplicity, one may still assume a photosphere that is located at a velocity much smaller than the 17,000 km s^{-1} as derived from the absorption minima of the P-cygni lines of Si II lines. The weaker S II "W" lines and Si III lines at 439.5 454.0, and 464.0 nm may provide a hint of the location of the photosphere. If so, at least along certain lines of sight the photosphere is at a velocity as low as 11,000 km s^{-1}. This rather low photospheric velocity may not be as surprising. From light curve fitting, we know that the pre-maximum luminosity of SN Ia rises approximately as t^2 (Goldhaber et al. 2001), which implies a photosphere at a fixed velocity if the atmosphere is approximated by a blackbody. A photospheric velocity of 11,000 km s^{-1} agrees with the observed luminosity and light curve behavior of typical SN Ia.

3.6. Similar Events

SN 1997bp and SN 2002bo displayed high velocity absorption features similar to those of SN 2004dt. Strong polarized features were also observed across the Si II 635.5 nm line for both SN 1997bp and SN 2002bo. Discussion of the polarization features of SN 1997bp and SN 2002bo will be given in a forthcoming paper. We discuss here only their distinct spectroscopic behavior. As pointed in Benetti et al. (2004), supernovae such as SN 1984A (e.g. Branch 1987) and SN 2002bo show unusually high velocity lines. A comparison of the spectra of SN 1997bp, SN 2002bo, SN 2004dt, and some spectroscopically normal SN Ia is shown in Figure 4. The characteristic behavior of SN 1997bp, SN 2002bo, and SN 2004dt is that they appear spectroscopically normal, but with the lines much broader and at much higher velocities. Benetti et al. (2004) suggest that for this group of supernovae the burning to silicon penetrated to higher layers than in more normal SN Ia. The high velocity, broad lines can be understood by the presence of a fast moving shell which is rich in intermediate mass elements and unburned oxygen. The extensions of this shell in velocity space requires detailed spectral modeling.

Both SN 1997bp, and SN 2002bo show strong narrow Na I D absorption that implies that they suffer considerable amount of dust extinction from the host galaxy. The equivalent widths of the Na I D absorption are 1.5 Å, and 2.5 Å for SN 1997bp, and SN 2002bo,

respectively. No strong Na I D line is detected for SN 2004dt. For SN 1984A, Barbon et al. (1989) derived $E(B-V) = 0.45 \pm 0.05$, Kimeridze & Tsvetkov (1986) found $A_B = 1.2 \pm 0.2$. Although these values are uncertain, the observed color around max does suggest large interstellar extinction. For SN 1997bp, Riess et al. (1998) give $A_V = 0.62$, suggesting $E(B-V) \approx 0.2$. A significant amount of dust along the light of sight of SN 1997bp in the host galaxy is also consistent with the presence of strong Na I D line. Benetti et al. (2004) found $E(B-V) = 0.43 \pm 0.10$ for SN 2002bo, in agreement with the observed strong Na I D in SN 2002bo. SN 2004dt does not show a noticeable Na I D line, and final light curves are not yet available to estimate the dust content on the line of sight. However, our flux calibrated spectrum shows $B-V \approx 0.07$ at day around -7, which implies an $E(B-V)$ of 0.14-0.2 when compared to colors of typical SN Ia at comparable epoch. These values of $E(B-V)$ are significantly larger than Typical values of $E(B-V)$ found for Type Ia supernovae (Knop et al. 2003).

It is not clear to us whether the extinction of these supernovae is caused by circumstellar or interstellar dust. High resolution spectroscopy may be helpful in this regard, but it may be difficult to use high resolution spectroscopy alone to tell whether the dust is within a few parsecs or a few hundred parsecs from the progenitor. Late time light echo observation (Patat 2004) combined with late time polarimetry may set more direct constraints on the location of the absorbing dust. A larger sample of SN 2004dt-like objects will resolve the issue of how strongly they are associated with dusty environments.

3.7. Continuum Polarization

We note that most of the discussion in this paper relies on polarization variations across spectral features, not on the level of continuum polarization. We will not elaborate on the geometrical structure of the photosphere. With the complicated geometry shown by the various lines, the continuum may be formed in a complicated clumpy environment. It is likely not to have a smooth geometry like the one assumed for ellipsoidal models.

Taking the adopted components of interstellar polarization at face value, we can see that the level of continuum polarization can be as low as 0.2-0.3%, consistent with what was found for SN 2001el. The amplitude of continuum polarization is larger in the red part of the spectrum, but with the sign of the polarization flipped. The polarization position angle at ~ 650 nm is 90 degrees different from that of the spectral lines and of the blue continuum at ~ 550 nm. Such a flip is expected if the symmetry axes of structures involved are the same, but with the geometry changed, for example from oblate to prolate. This may arise naturally as an optical depth effect as described in Höflich (1991) for a prolate geometry.

The exact level of continuum polarization awaits a full analysis of the data set which covers post-maximum phases of the supernovae.

4. Discussion and Conclusions

4.1. SN 20024dt and Other Polarized Supernovae

SN 2004dt continues to add to the data base that strongly suggests that SN Ia are polarized in a very interesting fashion, but with a variation from event to event that we are just beginning to probe.

SN 2004dt provides a unique opportunity to study the details of a Type Ia supernova. The observations have revealed both high and low velocity spectral features about a week before optical maximum. Strong variation of polarization across spectral lines of intermediate mass elements, especially silicon, is observed. On the other hand, no significant polarization signals are detected for the O I 777.4 nm feature. These characteristics provide important clues to the nature of this type of SN Ia especially high-velocity explosion.

SN 2004dt is different than SN 2001el. For the latter event, the strongest polarization feature was the high-velocity component of the Ca II IR triplet, Si II is polarized much lower level than Ca II IR triplet. For SN 2004dt, the polarization of the Ca II IR features is prominent, but polarizations of lines of Si II are the strongest. SN 2001el showed continuum polarization of the level of about 0.3%. SN 1996X tentatively showed similar levels of continuum polarization. As we discussed before, the precise level of continuum polarization of SN 2004dt is difficult to determine because of the highly-polarized spectral features. With the adopted level of interstellar polarization, the continuum level may be comparable to that of SN 2001el and SN 1996X; however, the large polarization across most of the spectral lines makes SN 2004dt distinctively different from SN 2001el. In Wang et al. (2003a), we speculated that it is important to study the correlations among the degree of polarization of the high velocity Ca II IR triplet, the strength of the high velocity component of the Ca II IR triplet, and the velocity of the Ca II IR triplet. The observations of SN 2004dt are consistent with a positive correlation between the strength of the high velocity Ca II IR triplet and the degree of polarization. The observations also seems to confirm the speculation that higher velocity events should show larger polarization. Obviously, more spectral polarization data are needed.

4.2. SN 2004dt and Sub-Types of SN Ia

All of the four Type Ia supernovae identified to have abnormally high velocity Si II lines show also evidence of unusually large reddening by the dust in the host galaxy. Both SN 1997bp and SN 2002bo are found to be significantly polarized, at levels around 1-2%. There were no polarimetry data on SN 1984A. This group of objects is likely to be characterized by high velocity, high dust extinction, and intrinsic large polarization before optical maximum.

We do not yet know whether these high velocity Type Ia supernovae form a separate sub-group of SN Ia, or whether they are simply a familiar sub-group of objects viewed at a special angle. For the latter possibility, SN 1991T-like events may be candidates to be their counterparts viewed at different angles. The only other sub-group of SN Ia that is known to be associated with dusty environments are SN 1991T-like events. Perhaps SN 1991T-like objects are viewed in a direction with very little intermediate mass elements in the outer layers, whereas SN 2004dt-like objects are the same objects viewed in the direction with substantial unburned elements on the outside.

4.3. Comments on Theoretical Models of Type Ia Supernova Explosions

SN Ia involve the combustion of a degenerate C/O white dwarf of the Chandrasekhar mass in a binary system (Whelan & Iben 1973; Nomoto 1980, 1982). Major theoretical questions concern the ignition and propagation of the flame through the white dwarf. Three major scenarios have been proposed: detonation (Arnett 1969; Hansen & Wheeler 1969), deflagration (Nomoto, Sugimoto, & Neo 1976; Nomoto, Thielemann, & Yokoi 1984), and delayed detonations (Khokhlov 1991; Yamaoka et al. 1992; Woosley & Weaver 1994). Three-dimensional calculations show that pure deflagration models leave unburned carbon and oxygen mixed into the center (Gamezo, Khokhlov & Oran 2002; Reinecke, Hillebrandt, Niemeyer, 2002). Delayed-detonation models leave very little unburned carbon and tend to produce the observed stratified composition structure (Gamezo, Khokhlov & Oran 2004; Marion et al. 2003; Höflich et al. 2001, 1995, Wheeler et al. 1998).

4.3.1. Deflagration

In SN 2004dt, we see a highly turbulent structure which extends from at least as deep as 11,000 km $s^{-1}$to at least 17,000 km s^{-1}. This turbulent structure could be consistent with those produced in 3-D simulations of deflagration models (Gamezo et al. 2002; Röpke,

Niemeyer, J. C., & Hillebrandt 2003). The layer at velocity around 17,000 km s^{-1} shows unburned oxygen and fragments of intermediate mass elements, but with no iron. Deeper inside, sulfur is found at a velocity around 11,000 km s^{-1} which shares the same asymmetry signature as the high velocity, oxygen-rich layer.

In deflagration models, silicon co-exists with iron; the absence of strong iron features in the spectrum may be inconsistent with published pure deflagration models, but we caution that the exact amount of iron that can be hidden in the spectra without producing pronounced spectral features is uncertain and quantitative spectral modeling is needed to set the constraints on deflagration models. The velocities of the silicon and magnesium are significantly higher than predicted by pure deflagration models. It thus seems that deflagration models are capable of producing the observed turbulent structure, but are perhaps incapable of producing the kinematics of the ejecta. Deflagration models may also have a problem with the absence of iron features in the ejecta. Deflagration models also predict unburned matter, C and O, mixed down to low velocities. Subsequent observations of this event will help to put constraints on this possibility. Deflagration models also tend to leave a layer of completely unburned C and O on the outside. It is very important to put limits on the amount of carbon in the spectra.

4.3.2. Delayed-Detonation

An alternative is the delayed-detonation (DD) model (Khokhlov 1991). This model assumes that at a certain stage of deflagration, the nuclear burning becomes supersonic and therefore switches to a detonation. In order to have a high velocity partially burned layer, there must be significant pre-expansion (due to the subsonic deflagration stage) before the onset of detonation, which sufficiently reduces the density of the progenitor white dwarf before the nuclear burning flame propagates to the surface layers. It may also be possible that there is a layer on the surface of the progenitor white dwarf with a density that is too low to burn at all. Because of the low density near the surface, the products of the nuclear reactions are mostly intermediate mass elements. A strong detonation wave is unlikely to generate a turbulent silicon layer such as we apparently observe in SN 2004dt. One possible way out is that the detonation wave weakens significantly near the surface of the star, in which case the cellular structure associated with detonation instability (Boisseau, et al. 1996; Gamezo et al. 1999) can grow to significant scales.

Alternatively, the detonation could be switched on at a stage where the deflagration flame has propagated sufficiently close to the low density part of the expanding white dwarf that the products of detonation bear the imprint of the complex structure of deflagration.

A delayed detonation would be able to boost the outer layers to the velocities we observe. It may also be consistent with the absence of iron features at very high velocity. Detailed modeling is needed in order to understand the turbulent structure of the products of nuclear burning.

4.3.3. Off-centered Delayed-Detonation

A different model which naturally produces a globally aspherical Type Ia is given in Livne (1999) in which the detonation is triggered at a point off the center of the white dwarf rather than in a spherical shell. The result is that the inner nickel region is offset from the centroid of the density distribution. The resulting off-center production of gamma-ray energy input can induce polarization even in a spherical density distribution (Chugai 1992; Höflich 1995). In addition, the silicon is predicted to be left with a distribution that is displaced from the centroid of the density distribution. This leads naturally to the possibility of a globally asymmetric silicon distribution that has the potential to produce significant polarization by large scale blocking of the photosphere as well as smaller scale clumps of silicon resulting from the turbulent burning. This sort of model thus has the capability of producing all the polarized signatures of the silicon-rich layer. Since the photosphere might also be significantly aspherical from the energy input or the asymmetric density distribution, a large continuum polarization may be produced by such a model - this should be confronted with detailed theoretical modeling. This model can be tested by spectroscopic observations in the nebular phase. We will defer a detailed discussion of this model to a later paper when the analysis of the complete data set of our observations is undertaken.

4.3.4. Gravitationally-Confined Detonation

In the model recently proposed by Plewa, Calder & Lamb (2004), the explosion begins as a deflagration born slightly off-center in the white dwarf. Buoyancy dominates the evolution of the deflagration, resulting in a very rapidly rising plume of burned material. This plume displaces the outer (unburned) layers of the star, which propagate ahead of burned bubble material across the surface of the star. This flow converges at the point opposite from where the plume emerges, and the resulting rapid compression of the unburned material triggers a detonation. An advantage of this model is that it may not require triggering the detonation artificially. This model has about 1 percent of a solar mass of iron group elements on the surface of the white dwarf resulting from the surface flow of the plume material. As for pure deflagration models, detailed spectroscopic modeling is needed to tell if this amount of iron

is allowed by observations. In addition, the requirement of significant pre-expansion so that sufficient intermediate mass elements are produced in the velocity range from 11,000 km s^{-1} to 25,000 km s^{-1} to match the observed spectra may further constrain this model. Note that pre-expansion is necessary to produce intermediate mass elements in the outer layers, but can significantly weaken the shock of the merging plume matter; this will work against the triggering of detonation. Therefore these observations will set limits on the parameter space where this mechanism may work. Due to pre-expansion at the stage of detonation, it is also possible that this mechanism will produce highly aspherical chemical structures such that one side (where detonation is triggered) consists of mainly iron rich material on the outside, whereas the otherside (where the burned bubble emerges) consists of mainly of intermediate mass elements. Depending on which side faces the observer, the target can appear as iron rich SN 1991T-like, or silicon rich SN 2004dt-like. However, the details of these constraints await thorough theoretical models of these data.

4.4. Implications on Cosmology

This study demonstrates the complicated nature of Type Ia supernovae. It shows the need for more detailed studies of Type Ia supernovae in order to make them better standard candles. Ability to identify peculiar events such as SN 2004dt, either photometrically or spectroscopically, is essential. Dividing Type Ia supernovae into sub-groups based on their spectral behavior may be an important task for future supernova cosmology experiments whose concerns are mostly systematic errors due to variations of intrinsic properties of supernovae.

There are two effects of asymmetry on the observed magnitudes of a supernova. First, asymmetry affects the total integrated light from a supernova in a particular filter, therefore causing a view-angle dependence of distances. Secondly, asymmetry will cause intrinsic color dispersions which can make the determination of color-excess due to dust in the host galaxy difficult. The second effect can become very important as errors on color are amplified when extinction corrections are to be applied.

The peculiar nature of events like SN 2004dt may require this group to be separated from other supernovae, and re-calibration of the methods (e.g. Phillips et al. 1999; Wang et al. 2003b) commonly used to derive distances and dust reddening of Type Ia supernovae.

The association with dusty environment suggests also that these events are likely to be from younger progenitor stars, and that they may be more abundant at higher red shifts than at our local universe. Identifying these events and applying the proper relations for

distance calibration is also critical in removing the effect of progenitor evolutions.

In summary, we have provided in this paper observations that may constrain various models of SN Ia explosions. More polarization observations will help to clarify these critical issues concerning SN Ia explosions. We stress that SN 2004dt may represent a particular sub-set of SN Ia, along with SN 1984A, SN 1997bp, and SN 2002bo, with especially high-velocity matter for which the explosion mechanism is significantly different from events with their lower velocity counterparts such as SN 1994D.

Acknowledgments: The authors are grateful to the European Southern Observatory for the generous allocation of observing time. They especially thank the staff of the Paranal Observatory for their competent and never-tiring support of this project in service mode. We are grateful to Tomesz Plewa for helpful discussions. The research of JCW is supported in part by NSF grant AST-0406740.

REFERENCES

Arnett, D. 1969, ApJ, 157, 1369

Barbon, R., Tijima, T., & Rosina, L. 1989, A&A, 220, 83

Benetti, S. et al. 2004, MNRaS, 348, 261

Boisseau, J. R., Wheeler, J. C., Oran, E. S., & Khokhlov, A. M. 1996, ApJ, 471, L99

Branch, D. 1987, ApJ, 316, L81

Chugai, N. N. 1992, SvAL, 18, 168

Gamezo, V. N., Khokhlov, A. M., & Oran, E. S. 2004, PHRvL, 92, 102

Gamezo, V. N., Khokhlov, A. M., Oran, E. S., Chtchelkanova, A. Y., & Rosenberg, R. O. 2002, Sci, 299, 71

Gamezo, V. N., Wheeler, J. C., Khokhlov, A. M., & Oran, E. S. 1999, ApJ, 512, 827

Gerardy, C. L., Höflich, P., Fesen, R. A., Marion, G. H., Nomoto, K., Quimby, R., Schaefer, B. E., Wang, L., & Wheeler, J. C. 2004, ApJ, 607, 391

Goldhaber et al. 2001, ApJ, 588, 359

Hasen, C. J., & Wheeler, J. C. 1969, Ap&SS, 3, 464

Höflich P. 1991 A&A, 246, 481

Höflich, P. 1995, ApJ, 440, 821

Höflich, P., Gerardy, C. L., Fesen, R. A., & Sakai, S. 2002, ApJ, 568, 791

Höflich, P., Khokhlov, A., Wheeler, J. C., Phillips, M. M., Suntzeff, N. B., & Hamuy, M. 1996, ApJ, 472, 81

Howell, D. A., Höflich, P., Wang, L., & Wheeler, J. C. 2001, ApJ, 556, 302

Hoyle, F. & Fowler, W. A. 1960, ApJ, 132, 565

Iben, I.J. & Tutukov, A.V. 1984, ApJ S 54 335

Khokhlov, A. M. 1991, A&A, 245, 114

Kimeridze, G. N., & Tsvetkov, D. Yu. 1986, Astrofizika 25, 279

Kirshner, R. P., et al. 1993, ApJ, 415, 589

Knop, R. et al. 2003, ApJ, 598, 102

Leonard, D. C., Filippenko, A. V., Ardila, D. R., & Brotherton, M. S. 2001, ApJ, 553, 861

Jeffery, D., Leibundgut, B., Kirshner, R. P., Benetti, S., Branch, D., & Sonneborn, G. 1992, ApJ, 397, 304

Livne, E. 1999, ApJ 527, L97

Marietta, E., Burrows, A., & Fryxell, B. 2000, ApJS, 128, 615

Marion, G. H., Höflich, P., Vacca, W. D., & Wheeler, J. C 2003, 591, 316

Moore, M. & Li, W. 2004, IAUC 8386

Nomoto, K. 1980, ApJ, 248, 798

Nomoto, K. 1982, ApJ, 257, 78

Nomoto, K., Sugimoto, D., & Neo, S. 1976, Ap&SS, 39, L37

Nomoto, K., Thielemann, F.-K., & Yokoi, K. 1984, ApJ, 286, 644

Patat, F., Benetti, S., Cappellaro, E., Danziger, I. J., Della Valle, M., Mazzali, P. A., & Turatto, M. 1996, ApJ, 278, 111

Patat, F. 2004, MNRaS, submitted

Patat, F., Pignata, G. & Benetti, S. 2004, IAUC 8387

Phillips, M. M., Lira, P., Suntzeff, N., B., Schommer, R. A., Hamuy, M., & Maza, J. 1999, 118, 1766

Plewa, T., Calder, A. C., & Lamb, D. Q. 2004, ApJ, 612, L37

Reinecke, M., Hillebrandt, W., & Niemeyer, J. C. 2002, A&A, 391, 1167

Riess, A. G., Nugent, P. E., Filippenko, A. V., Kirshner, R. P., & Perlmutter, S. 1998, ApJ, 504, 935

Röpke, F. K., Niemeyer, J. C., & Hillebrandt, W. 2002, A&A, 588, 952

Salvo, M., Schmidt, B. & Wood, P. 2004, IAUC 8387

Schlegel, D. J., Finkbeiner, D. P., & Davis, M. 1998, ApJ, 500, 525

Wang, L. 2003, Proceedings of the Workshop on 3-D Signatures in Stellar Explosions, Austin, Texas, in the press, astro-ph/0311299

Wang, L., Baade, D., Höflich, P., Khokhlov, A., Wheeler, J. C., Kasen, D., Nugent, P. E., Perlmutter, S., Fransson, C., & Lundqvist, P. 2003a, ApJ, 591, 1110

Wang, L., Baade, D., Höflich, P., Wheeler, J. C., Kawabata, K., & Nomoto, K. 2004, ApJ, 604, L53

Wang, L., Goldhaber, G., Aldering, G., & Perlmutter, S. 2003b, ApJ, 590, 944

Wang, L., Howell, D. A., Höflich, P., & Wheeler, J. C. 2001, ApJ, 550, 1030

Wang, L., & Wheeler, J. C. 1997, IAUC, 6222

Wang, L., Wheeler, J. C., & Hoeflich, P. 1997, ApJ, 476, L27

Wang, L., Wheeler, J. C., Höflich, P., Khokhlov, A., Baade, D., Branch, D., Challis, P., Filippenko, A. V., Fransson, C., Garnavich, P., Kirshner, R. P., Lundqvist, P., McCray, R., Panagia, N., Pun, C. S. J., Phillips, M. M., Sonneborn, G., Suntzeff, N. B. 2002, ApJ, 579, 671

Wang, L., Wheeler, J. C., Li, Z., & Clocchiatti, A. 1996, ApJ, 467, 435

Wheeler, J. C. & Harkness, R. P. 1990, RPPH, 53, 1467

Wheeler, J. C., Höflich, P., Harkness, R. P., & Spyromilio, J. 1998, ApJ, 496, 908

Whelan, J. & Iben, I. J. 1973, ApJ, 186, 1007

Woosley, S. E., & Weaver, T. A. 1994, ApJ, 420, 348

Yamaoka, H., Nomoto, K., Shigeyama, T., & Thielemann, F. 1992, ApJ, 393, L55

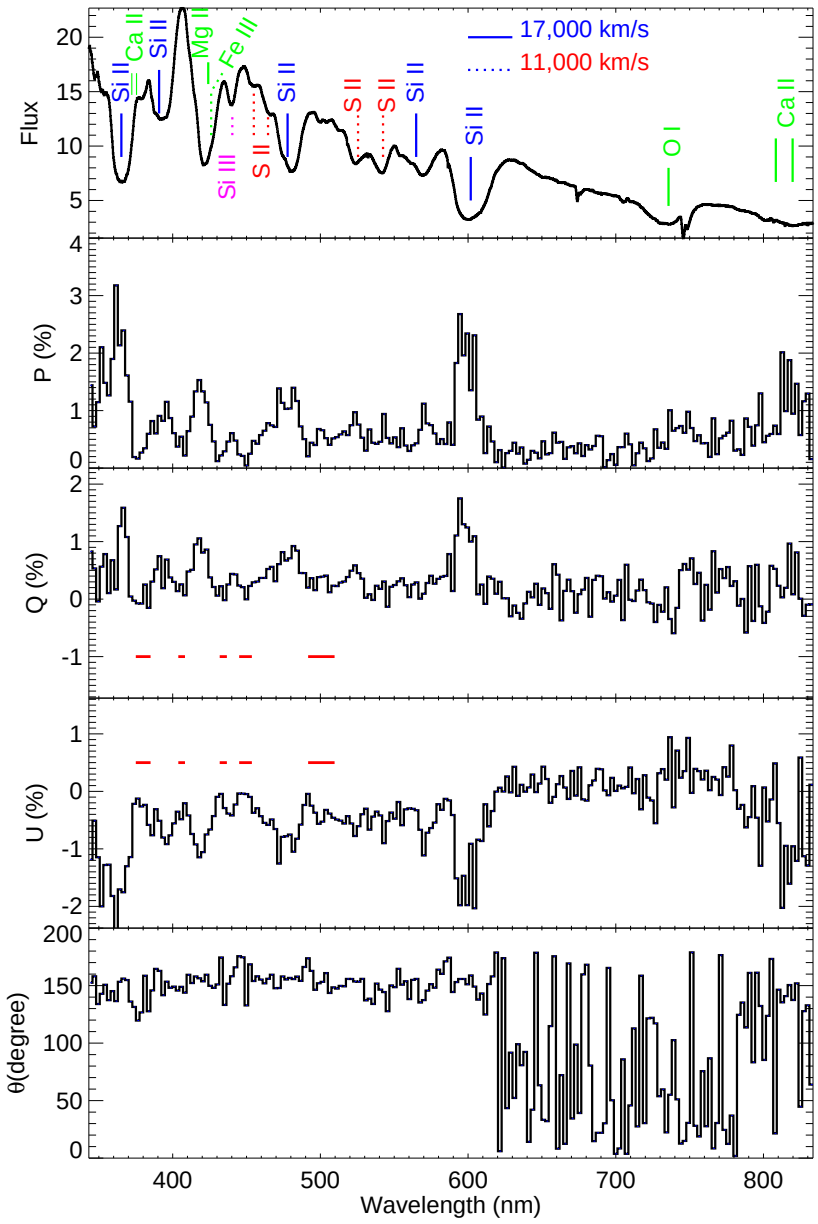

Fig. 1.— Spectroscopy of SN 2004dt de-redshifted assuming a recession velocity of 5915 km s^{-1} of the host galaxy. The four panels give the total flux spectrum, the polarization, P, the Stokes vectors, Q and U and the polarization angle θ. Typical spectral features are marked on the top pannel. The lines are produced by material moving at velocities of 17,000 km s^{-1} (marked by solid lines) and 11,000 km s^{-1} (marked by dotted lines; see Fig. 3 for a more complete description) in the rest frame of the supernova. Lines from different elements are marked with different colors (gray scales). The pannels for polarization data are binned to 25 Å. The wavelength regions used to determine interstellar polarization are marked by horizontal lines on the pannels for Q and U. Stronger lines tend to be associated with larger degrees of polarization except for the O I 777.4 nm line.

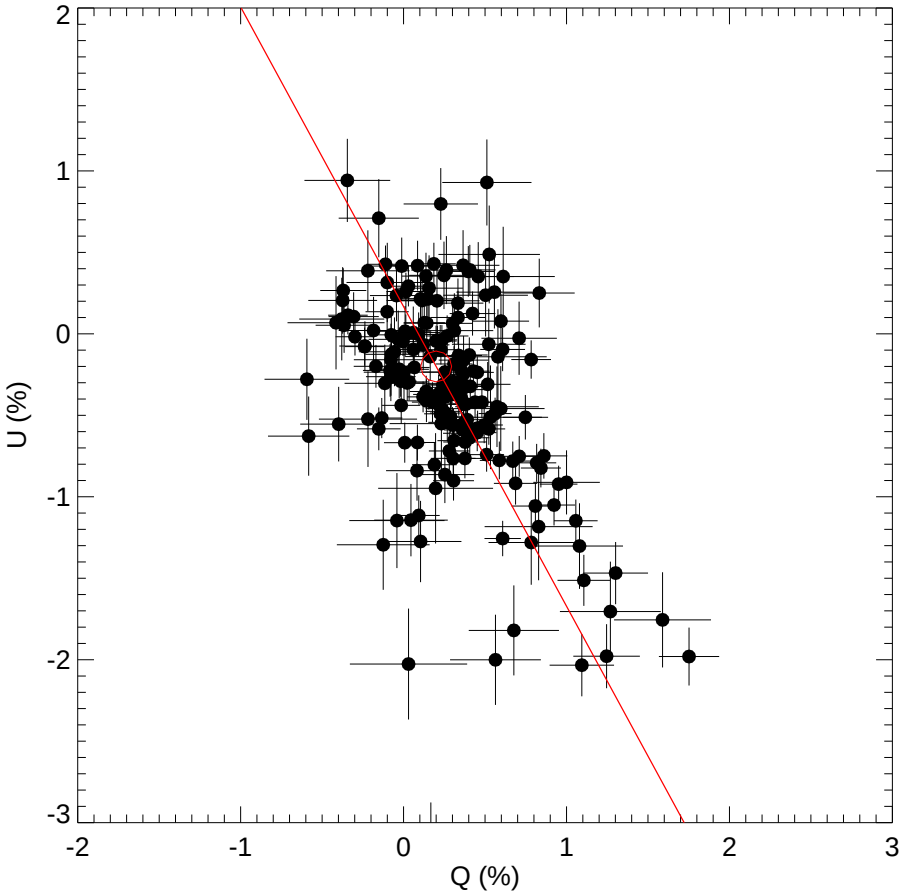

Fig. 2.— Spectropolarimetry of SN 2004dt displayed in the plane of the Stokes vectors Q and U. Note the existence of a dominant axis represented by the solid line. The 1-σ location of the polarization due to interstellar dust is shown as an open circle. The data points are binned to 25 Å.

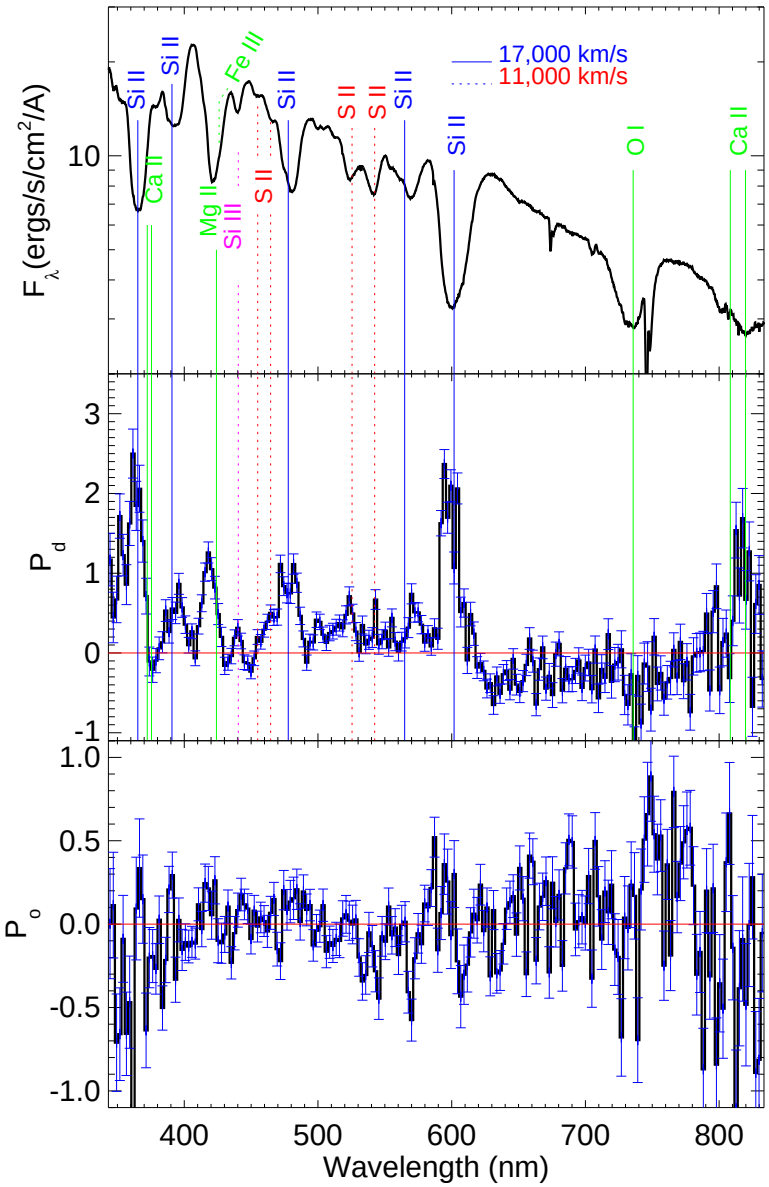

Fig. 3.— The top panel gives the total flux spectra; the next two panels give the polarization spectrum projected onto the dominant axis and the orthogonal axis, respectively. The solid vertical lines mark the positions of the lines of Si II, Mg II, Ca II, and O I which are typically blue shifted by 17,000 km s^{-1}. The vertical dash lines mark the positions of the lines of S II, Si III, and Fe III, at a blue shift of 11,000 km s^{-1}. All the polarized features except O I line share the same dominant axis, suggesting that the geometrical structures of Si II, Mg II, and Ca II are the same. No polarization is detected across the O I line. Weaker lines of Si III, and S II show also polarization along the dominant axis. The data are binned to 25 Å. Note that the polarization features at 747.0 nm may not be reliable because of telluric absorption.

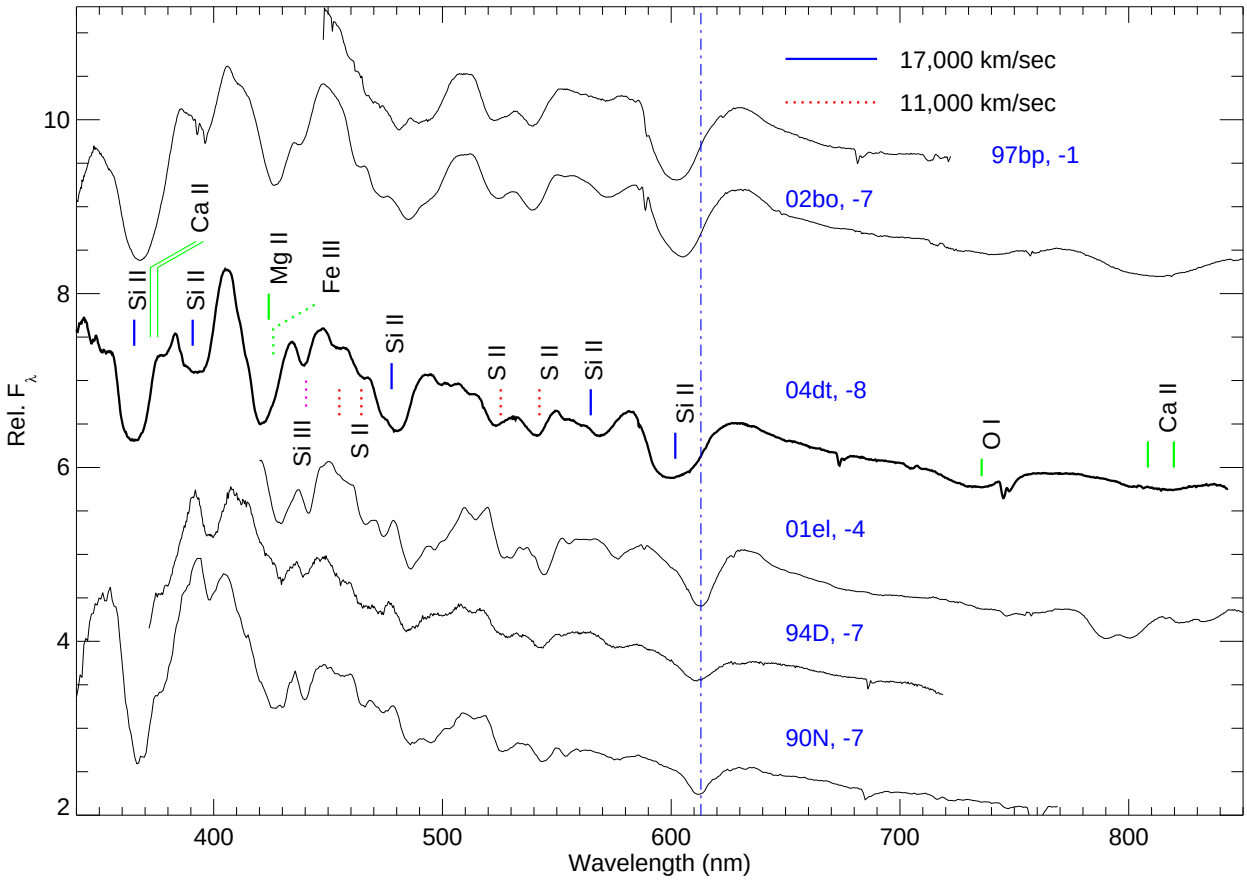

Fig. 4.— Comparisons of spectra of SN 1997bp, SN 2002bo, SN 2004dt, SN 1990N, SN 1994D, and SN 2001el before optical maximum. The data of SN 1997bp were obtained at the 2.1 meter telescope of McDonald Observatory through our program of supernova polarimetry (Wang & Wheeler 1997). The data on SN 2002bo and SN 2001el were obtained by our supernova polarimetry program at the VLT (Wang et al. 2003a). The data of SN 1994D is from Patat et al. (1996). The data of SN 1990N is from Jeffery et al. (1992). The Si II 635.5 nm lines of SN 1997bp, SN 2002bo, and SN 2004dt are significantly broader than those of SN 1990N, SN 1994D, and SN 2001el around optical maximum. The vertical line marks the absorption minimum of the Si II 635.5nm line of SN 2001el, SN 1994D, and SN 1990N. The Si II 635.5nm lines of SN 1997bp, SN 2002bo, SN 2004dt show significantly larger blue shift than those of SN 2001el, SN 1994D, and SN 1990N.